Clinical Extrapolation of the Effects of Dolutegravir and Other HIV Integrase Inhibitors on Folate Transport Pathways

Maciej J. Zamek-Gliszczynski*, Xuexiang Zhang*, Jennypher Mudunuru, Yewei Du, Jian-Lu Chen, Kunal S. Taskar, Jane Huang, Yong Huang, and Elizabeth H. Romach

GlaxoSmithKline, Collegeville, PA, USA (MJZ-G, JM), and Ware, UK (KST); BioIVT, Santa Clara, CA, USA (XZ, YD, J-LC, JH, YH); ViiV Healthcare, RTP, NC, USA (EHR)

*Authors contributed equally to this work

Running Title: Integrase inhibitor effects on folate transport (48/80 characters)

Corresponding Author:

Maciej J. Zamek-Gliszczynski, Ph.D.

GlaxoSmithKline

1250 South Collegeville Rd

Collegeville, PA 19426, USA

e-mail: maciej.x.zamek-gliszczynski@gsk.com

Tel: 1-610-270-6278

Number of text pages: 32

Number of Figures: 6

Number of Tables: 1

References: 39

Abstract: 250/250

Significance Statement: 118/120

Introduction: 681/750

Discussion: 1,500/1,500

Abbreviations: neural-tube defects (NTDs), proton-coupled folate transporter (PCFT), reduced folate carrier (RFC), folate receptor α (FRα), dihydrofolate reductase (DHFR), Madin-Darby Canine Kidney-II (MDCK-II), inhibitory concentration (IC)

Abstract (250/250 words)

Preliminary analysis of ongoing birth surveillance study identified evidence of potential increased risk for neural-tube defects (NTDs) in newborns associated with exposure to dolutegravir at time of conception. Folate deficiency is a common cause of NTDs. Dolutegravir and other HIV integrase inhibitor drugs were evaluated *in vitro* for inhibition of folate transport pathways: proton-coupled folate transporter (PCFT), reduced folate carrier (RFC), and folate receptor α (FRα)-mediated endocytosis. Inhibition of folate transport was extrapolated to clinic using established approaches for transporters in intestine, distribution tissues, basolateral and apical membranes of renal proximal tubules (2017 FDA Guidance). The positive controls methotrexate and pemetrexed demonstrated clinically-relevant inhibition of PCFT, RFC, and FRα in folate absorption, distribution, and renal sparing. Valproic acid was used as negative control that elicits folate-independent NTDs; valproic acid did not inhibit PCFT, RFC, and FRα. At clinical doses/exposures, observed *in vitro* inhibition of FRα by dolutegravir and cabotegravir was not flagged as clinically relevant; PCFT and RFC inhibition was not observed *in vitro*. Bictegravir inhibited both PCFT and FRα, but the observed inhibition did not reach the criteria for clinical relevance. Elvitegravir and raltegravir inhibited PCFT, but only raltegravir inhibition of intestinal PCFT was flagged as potentially clinically-relevant at the highest 1.2g dose (not 400mg dose). These studies showed that dolutegravir is not a clinical inhibitor of folate transport pathways, and it is not predicted to elicit clinical decreases in maternal and fetal folate levels. Clinically-relevant HIV integrase inhibitor drug class effect on folate transport pathways was not observed.

Significance Statement (118/120 words)

Preliminary analysis of ongoing birth surveillance study identified evidence of potential increased risk for neural-tube defects (NTDs) in newborns associated with exposure to the HIV integrase inhibitor, dolutegravir, at time of conception; folate deficiency is a common cause of NTDs. Dolutegravir and other HIV integrase inhibitor drugs were evaluated *in vitro* for inhibition of the major folate transport pathways: proton-coupled folate transporter (PCFT), reduced folate carrier (RFC), and folate receptor α (FRα)-mediated endocytosis. The present studies showed that dolutegravir is not a clinical inhibitor of folate transport pathways, and it is not predicted to elicit clinical decreases in maternal and fetal folate levels. Furthermore, clinically-relevant HIV integrase inhibitor drug class effect on folate transport pathways was not observed.

Introduction (681/750 words)

Dolutegravir is an integrase inhibitor for the treatment of HIV, a drug class that also includes bictegravir, elvitegravir, raltegravir, and cabotegravir, which is completing Phase III trials (Han et al., 2017). Preliminary analysis of an ongoing birth surveillance study identified evidence of a potential increased risk for neural-tube defects (NTDs) in newborns associated with exposure to dolutegravir at the time of conception (Zash et al., 2018). This observation was unexpected, because standard pre-clinical reproductive toxicity studies in rats and rabbits did not identify fetal abnormalities at exposures up to 27-fold higher than at the maximum recommended human dose (Tivicay Prescribing Information, 2018).

Folate is critical to proper neural tube embryonic development in the first four weeks of human pregnancy (Botto et al., 1999). Women of child-bearing potential are therefore encouraged to supplement folic acid (Botto et al., 1999; Kancherla et al., 2018). Since neural tube development occurs before most women know they are pregnant, many countries implemented folate fortification of the food via wheat and/or maize flour supplementation (Kancherla et al., 2018). Likewise, rodent chow of laboratory animals is supplemented with folate, as these animals have no access to natural vitamin sources. Notably the food supply is not fortified with folate in Botswana, where the dolutegravir birth surveillance study was conducted (Kancherla et al., 2018; Zash et al., 2018).

Drug-induced folate deficiency leading to increased incidence of adverse effects including neurotoxicity and embryonic NTDs, as well as rescue/prevention with folate supplementation are well established for the anti-folate drug methotrexate (DeSesso and Goeringer, 1991; Cohen, 2017). Likewise, the intravenous anti-folate pemetrexed is indicated for use only with folate pre-medication and over-supplementation to avoid serious toxicities

associated with folate depletion in cancer patients (Alimta Prescribing Information, 2019).

However, folate deficiency is not the sole cause of increased NTD risk associated with drug

treatment. For example, the antiepileptic drug, valproic acid, increases the incidence of NTDs

four-fold relative to other antiepileptic therapies used in pregnant women (Depakene Prescribing

Information, 2011). As folate supplementation does not reduce the incidence of valproic acid

NTDs, this drug is considered to elicit NTDs via unknown folate-independent mechanism(s)

(Hansen et al., 1995; Craig et al., 1999; Candito et al., 2007).

Folate's hydrophilic nature results in negligible passive membrane permeability and

transport-mediated disposition. Transport mechanisms governing folate intestinal absorption,

distribution, and renal sparing are depicted in Figure 1 (Kim et al., 2004; Solanky et al., 2010;

Zhao et al., 2011). The proton-coupled folate transporter (PCFT), a solute carrier family

transporter, is primarily responsible for folate intestinal absorption. Distribution of folate into

the tissues, including the placenta and brain, involves the solute carriers PCFT and reduced folate

carrier (RFC), as well as folate receptor α (FRα)-mediated endocytosis. Like other hydrophilic

nutrients/vitamins, folate is not bound to plasma protein in blood, and therefore undergoes

extensive glomerular filtration in the kidney. Since folate passive tubular reabsorption is

negligible due to low permeability, folate requires efficient tubular reabsorption (a.k.a. renal

sparing), so that blood folate is not rapidly excreted in urine (Zhao et al., 2011). All three folate

transport processes are involved in folate active tubular reabsorption.

Another mechanism of folate deficiency is inhibition of dihydrofolate reductase (DHFR),

which converts dietary folic acid into reduced folates used for nucleic and amino acid synthesis.

Dolutegravir is not an inhibitor of DHFR (Cabrera et al., 2019), and since this mechanism has

already been ruled out, the present study focused on folate transport.

6

HIV integrase inhibitors were evaluated for inhibition of PCFT folate transport, RFC transport of reduced folate, and FRα-mediated folic acid endocytosis. Inhibition of these folate transport pathways was investigated *in vitro* and was extrapolated to clinic using established approaches based on regulatory recommendations for drug-drug interactions for transport processes in intestine, distribution tissues, basolateral and apical membranes of the renal proximal tubules (FDA, 2017). The aim of this work was to determine whether dolutegravir is a clinically-relevant inhibitor of the three major folate transport pathways, which could increase the risk maternal and/or fetal folate deficiency and NTDs, as well as to investigate potential HIV integrase inhibitor drug class effect on folate transport.

7

Materials and Methods

Materials

Dolutegravir and cabotegravir were provided by GlaxoSmithKline (Zebulon, NC). Bictegravir

was purchased from Medkoo Biosciences (Morrisville, NC). Raltegravir and elvitegravir were

obtained from Cayman Chemical (Ann Arbor, MI). Methotrexate, pemetrexed, valproic acid,

and bromosulfophthalein were purchased from Sigma-Aldrich (St. Louis, MO). [^{3}H]-folic acid

and [^{3}H]-methotrexate were purchased from Moravek (Brea, CA). All other chemicals were of

reagent grade and readily available from commercial sources.

Folate transport assays

The test system was Madin-Darby Canine Kidney-II (MDCK-II) cell polarized monolayers

grown on permeable supports of 96-well transwell plates. The MDCK-II cells were individually

transfected to express PCFT, RFC, FRα, or vector control transiently.

Assay conditions for PCFT, RFC, FRα are summarized in Figure 2. PCFT is expressed

on the apical membrane in the kidney/MDCK-II renal cell line (Zhao et al., 2011), hence all

incubations in this study were done on the apical side. The test article was pre-incubated for 30

minutes at pH 7.4 on the apical side to account for potential time-dependent inhibition and to

allow test article to equilibrate with cells followed by a 5-minute co-incubation of 10 nM [^{3}H]-

folic acid with the test article at pH 5.5 (PCFT co-transports folic acid with a proton). Folic acid

uptake in PCFT versus vector control cells was determined. Samples for test article

concentration and lactate dehydrogenase were collected from the apical side.

RFC is localized on the basolateral membrane kidney/MDCK-II renal cell line (Zhao et

al., 2011), thus all test article incubations were done on the basolateral side (see Figure 2B).

8

RFC is the reduced folic acid carrier and does not transport folic acid, but its reduced forms; 0.5 µM [³H]-methotrexate was used as a reduced form of folate in these studies (Mauritz et al., 2001). The 30-min pre-incubation and 5 min co-incubation were similar to PCFT, except the pH of the medium for RFC experiments was 7.4 during co-incubation (RFC activity is optimal at neutral pH) (Matherly et al., 2007; Zhao et al., 2011). Methotrexate cellular uptake in RFC versus vector control cells was determined. Samples for test article concentration and lactate dehydrogenase were collected from the basolateral side.

FRα is expressed on both apical and basolateral membranes of the MDCK-II renal cell line (Kim et al., 2004). As such, test articles were incubated on both apical and basolateral sides (see Figure 2C). Pre-incubation with test article (30 min) was followed by a 2-hour co-incubation of 50 nM [³H]-folic acid with the test article at pH 7.4. Folic acid cellular uptake in FRα cells versus the vector control cells was determined. Samples for test article concentration were collected from both basolateral and apical sides; LDH leakage was measured only on the apical side.

Specific transport activity was determined by subtraction of mean cellular uptake in vector control cells (incubated at the same time under same conditions) from that observed in PCFT, RFC, or FRα overexpressing cells (n = 4 wells/cell type/condition). Nominal test drug concentration ranges started at the highest soluble concentration based on visual inspection and were decreased in half-log increments for a total of eight concentrations: 0.03 to 100 µM for dolutegravir, cabotegravir, elvitegravir and 0.3 to 1000 µM for bictegravir, raltegravir, methotrexate, pemetrexed, and valproic acid. Actual test drug concentrations at the end of experiment were measured and used for determination of all inhibitory concentrations (see sample analysis and data analysis sections below).

The following criteria were used to deem transport/endocytosis activity acceptable in any assay run: 1) PCFT-mediated folic acid uptake: $\geq$31.6 fmol/min/cm^2, RFC-mediated methotrexate uptake: $\geq$46.3 fmol/min/cm^2, FRα-mediated folic acid endocytosis: $\geq$4.51 fmol/min/cm^2, and 2) $\geq$70% inhibition of transporter-mediated uptake or receptor-mediated endocytosis by prototypical inhibitors: 300 µM bromosulfophthalein for PCFT-mediated folic acid uptake, 1000 µM pemetrexed for RFC-mediated methotrexate uptake, 300 µM pemetrexed for FRα-mediated folic acid.

Sample analysis

The transport or endocytosis of each assay substrate was determined by radiometric detection. In the transport and endocytosis studies, the concentrations of test articles from the donor sides at the end of co-incubation were measured by LC/MS/MS (see Supplemental Methods 1 for summary of LC/MS/MS methods). These measured concentrations were used in the calculation of all inhibitory concentrations (except second positive control, pemetrexed, for which nominal concentrations were used). Potential cytotoxicity was evaluated by the release of lactate dehydrogenase, whose activity was quantified by spectrophotometric quantification (λ = 590 nm) of formazan formation using a commercial kit (G-Biosciences, St. Louis, MO).

Data analysis

In vitro data analysis

Net transporter- or receptor-mediated uptake activity (fmol/min/cm^2)

= [(accumulation in overexpressing cells) - (accumulation in control cells)]

/ [substrate incubation time * transwell insert surface area]

10

Percent transporter- or receptor-mediated uptake activity

$$= 100 - [100 * (\text{net uptake activity}_{\text{with inhibitor}} / (\text{net uptake uptake activity}_{\text{without inhibitor}})]$$

Inhibitory concentration (IC)

Inhibitory concentration 50 (IC_{50}) values were estimated by non-linear least squares fitting of the

following equation to the uptake data (GraphPad Prism v.5, San Diego, CA):

$$\text{uptake activity}_{\text{inhibitor concentration}} = \text{uptake activity}_{\text{no inhibitor}} / [1+ ([\text{Inhibitor Concentration}]/IC)^n]$$

where n is the Hill coefficient. Wherever $\geq 50\%$ inhibition was achieved, the associated

inhibitory concentration (IC_{50}) values are reported. Otherwise, the greatest extent of inhibition

observed $\geq 25\%$ is reported and discussed. This $\geq 25\%$ inhibition level was selected on the basis

that $\geq 25\%$ cumulative inhibition of folate absorption, distribution, and renal tubular reabsorption

(sparing) would decrease fetal folate levels >2-fold (Zamek-Gliszczynski et al., 2009; Zamek-

Gliszczynski et al., 2013).

Percent cytototoxicity

$$= (\text{LDH}_{\text{inhibitor concentration}} - \text{LDH}_{\text{vehicle control}}) / (\text{LDH}_{\text{1\% Tritox-X}} - \text{LDH}_{\text{vehicle control}}) * 100\%$$

Where LDH = lactate dehydrogenase. Lactate dehydrogenase activity at any given inhibitor

concentration had to be statistically significant (t-test with Bonferroni correction) vs. vehicle

control, and percent cytotoxicity had to be >12.5% (>half of minimal inhibition level considered

in this study) to disqualify uptake inhibition data due to confounding cytotoxicity.

Clinical extrapolation

Since clinical extrapolation of *in vitro* nutrient-drug transport inhibition is not well established,

clinical extrapolation of observed *in vitro* inhibitory potency values was based on established

thresholds (FDA, 2017). This extrapolation framework is considered the best available and

11

considers the worst-case scenario, although it was validated for drug-drug interactions, and not drug-folate interactions with the transport pathways studied herein specifically.

Intestinal Absorption:

Cut-off: Igut/IC ≥ 10

where, Igut = highest clinical dose / 250 mL or maximal aqueous solubility; IC = inhibitory concentration eliciting noted percentage of inhibition (50% or ≥25% for the purpose of this study)

Distribution:

Cut-off: 1+Cmax,u/IC ≥ 1.1

Proximal Tubule Reabsoprtion (apical proximal tubule transport pathways: PCFT and FRα):

Cut-off: 1+Cmax,u/IC ≥ 1.02

Proximal Tubule Reabsoprtion (basolateral proximal tubule transporter: RFC):

Cut-off: 1+Cmax,u/IC ≥ 1.1

where, Cmax,u = unbound plasma Cmax at highest clinical dose; IC = Inhibitory concentration eliciting noted percentage of inhibition (50% or ≥25% for the purpose of this study)

Data presentation

All data are reported as mean ± standard deviation (n = 4 replicates), unless otherwise noted. Statistical significance was assessed by student's *t*-test with Bonferroni's correction for multiple comparisons. All reported inhibitory concentrations refer to experimentally-determined concentrations measured at the end of the co-incubation period in the MDCK-II assays (except second positive control, pemetrexed, for which nominal concentrations were used).

Results

Functional verification of optimized folate *in vitro* transport assays (Figure 2) is summarized in Supplemental Figure 2. Briefly, PCFT functional activity was confirmed with folic acid uptake that was on average 31.7-fold (CV = 18.3%, n = 3 independent experiments) enhanced in PCFT vs. vector control cells. RFC did not transport un-reduced folic acid in this experimental system (data not shown), consistent with literature (Mauritz et al., 2001). Instead, methotrexate was selected as a reduced form of folic acid and demonstrated 2.1-fold (CV = 21.7%, n = 3 independent experiments) enhanced cellular uptake in RFC vs. vector control cells. This relatively lower magnitude of RFC functional enhancement in overexpressing cells has been reported previously (Kneuer et al., 2005), and emphasizes the importance of vector-control cell activity correction to determine overexpressed RFC activity. FRα-mediated folic acid endocytosis was 10.7-fold (CV = 16.9%, n = 3 independent experiments) enhanced in FRα overexpressing vs. vector control cells ($1.2\text{-}1.3 \times 10^5$ FRα mRNA overexpression was confirmed by PCR; data not shown). Prototypical inhibitors, bromosulfophthalein for PCFT (Nakai et al., 2007) and pemetrexed for RFC and FRα (Chattopadhyay et al., 2007), inhibited these respective folate transport pathways in a concentration-dependent manner (IC_{50} = 78.1 ± 7.5 µM, 157 ± 24 µM, and 17.5 ± 1.4 µM for PCFT, RFC, and FRα, respectively), with nearly complete inhibition at the highest 1 mM inhibitor concentration (Supplemental Figure 2).

PCFT inhibition results are summarized in Figure 3. The clinical positive control, methotrexate inhibited PCFT (IC_{50} = 2.9 ± 0.3 µM); in contrast, no inhibition was observed for the clinical negative control, valproic acid (Fig. 3B-C). Dolutegravir and cabotegravir at all test concentrations (up to maximum soluble in assay buffer) did not inhibit PCFT (Fig. 3D-E). Bictegravir inhibited PCFT (IC_{50} = 370 ± 23 µM; Fig. 3F). Elvitegravir elicited 28.1 ± 3.3%

PCFT inhibition at 30.0 ± 2.0 µM, and raltegravir inhibited PCFT $32.4 \pm 2.4\%$ at 564 ± 38 µM (Fig 3G-H).

RFC inhibition results are summarized in Figure 4. The clinical positive control, methotrexate inhibited RFC ($IC_{50} = 0.08 \pm 0.03$ µM); no inhibition was noted for the clinical negative control, valproic acid (Fig. 4B-C). The five integrase inhibitors drugs did not inhibit RFC transport (Fig 4D-H) at any concentration tested, up to the maximum soluble in assay buffer.

Inhibition of FRα-mediated folic acid endocytosis is summarized in Figure 5. The clinical positive control, methotrexate inhibited FRα ($IC_{50} = 50.4 \pm 5.3$ µM); inhibition exceeding the 25% pre-defined threshold for this study was not observed for the clinical negative control, valproic acid (Fig. 5B-C). Dolutegravir inhibited FRα $36.0 \pm 5.7\%$ at 37.3 ± 4.2 µM, and cabotegravir inhibited FRα $36.7 \pm 5.8\%$ at 25.8 ± 5.0 µM (Fig. 5D-E). Bictegravir inhibited folic acid FRα-mediated endocytosis with an IC_{50} of 268 ± 66 µM (Fig. 5F). Although elvitegravir elicited an apparent 14-38% decrease in FRα-mediated folic acid cellular accumulation at the top two concentrations tested, this decrease was comparable in magnitude to 14-27% cytotoxicity observed at these elvitegravir concentrations in this assay (Supplemental Table 3); therefore, no apparent inhibition of FRα by elvitegravir was concluded. Raltegravir did not inhibit FRα (Fig. 4H).

Drug parameters necessary for clinical extrapolation of *in vitro* folate transport inhibition results are presented in Table 1. Clinical extrapolations of PCFT, RFC, and FRα inhibition in folate intestinal absorption, distribution, and renal tubular reabsorption are summarized in Figure 6. Extrapolations for folate intestinal absorption were only made for PCFT, because the other

two pathways are not involved in this process, while all three pathways are involved in folate

distribution and renal sparing (Figure 1).

The anti-folate drugs, methotrexate and pemetrexed, were flagged as clinically-relevant

inhibitors of PCFT, RFC, and FRα in folate absorption, distribution, and renal tubular

reabsorption (Figure 6; FDA, 2017). Inhibition of PCFT transport of folic acid by bictegravir,

raltegravir, and elvitegravir was only flagged as potentially clinically-relevant for 1,200 mg oral

raltegravir in intestinal folate absorption ($Igut/IC_{32} > 10$). Otherwise, 400 mg oral raltegravir did

not meet the criteria for clinically-relevant intestinal PCFT inhibition; bictegravir, raltegravir,

and elvitegravir were not clinically-relevant systemic PCFT inhibitors in folate distribution and

renal tubular reabsortion (Figure 6; FDA, 2017). None of the five HIV integrase inhibitor drugs

were considered to be clinical inhibitors of RFC, because *in vitro* RFC inhibition was not

observed up to their respective maximal soluble concentrations, which were sufficiently high to

rule out intestinal and systemic inhibition at clinical doses and exposures (Table 1). Inhibition of

FRα-mediated folic endocytosis by dolutegravir, cabotegravir, and bictegravir observed *in vitro*

was well below the thresholds for potential clinical relevance of transport pathways at the level

of tissue distribution (1+Cmax,u/IC << 1.1) and renal tubular reabsorption on apical membrane

of renal proximal tubules (1+Cmax,u/IC << 1.02) (Figure 6; FDA, 2017).

Discussion (1,500/1,500 words)

Preliminary analysis of an ongoing clinical birth surveillance study suggested increased risk of NTDs in newborns from mothers taking dolutegravir at time of conception (Zash et al., 2018). Dolutegravir is an integrase inhibitor for the treatment of HIV, a drug class that also includes cabotegravir, bictegravir, raltegravir, and elvitegravir (Han et al., 2017). Folate deficiency increases the incidence rate of NTDs (Daly et al., 1995; Botto et al., 1999; Crider et al., 2014; Kancherla et al., 2018). Folate relies on transport via PCFT for intestinal absorption, FRα-mediated endocytosis along with transport by PCFT and RFC for tissue distribution, including to the fetus, and renal sparing via active tubular re-absorption following extensive glomerular filtration (Figure 1, Solanky et al., 2010; Zhao et al., 2011).

The aim of the present work was to determine whether dolutegravir and other integrase inhibitor drugs may be clinically-relevant inhibitors of the three major folate transport pathways, which would support increased likelihood of folate deficiency leading to increased NTD risk. Of the five HIV integrase inhibitor drugs evaluated for inhibition of PCFT, RFC, and FRα in folate absorption, distribution, and renal tubular reabsorption, only raltegravir at the highest 1.2g clinical dose was flagged as a potential clinical inhibitor of PCFT intestinal folate absorption. Otherwise, these five HIV integrase inhibitor drugs are not predicted to be inhibit the three major folate transport pathways at known clinical therapeutic concentrations (Figure 6; FDA, 2017).

Based on the current results, dolutegravir is not predicted to elicit clinical decreases in maternal and fetal folate levels. Furthermore, dolutegravir is not an inhibitor of DHFR, the first step in folic acid metabolism in synthesis of nucleic and amino acids (Cabrera et al., 2019). Taken together, these results do not support dolutegravir-induced folate deficiency as a mechanistic explanation for the reported preliminary observations of increased NTD risk (Zash

16

et al., 2018). As such, these studies do not lend mechanistic support for folate supplementation to overcome this proposed increased NTD risk (Zash et al., 2018). However, there is no harm to folate supplementation, and it is an established good practice known to reduce the risk of NTDs in the general population who may not otherwise consume adequate amounts of dietary folate (Botto et al., 1999; Kancherla et al., 2018). Although studies repeatedly failed to demonstrate folate supplementation to reduce the 4-fold increased NTD rate in epileptic women on valproic acid treatment, folate supplementation is still recommended for women of child bearing potential taking valproic acid as a safe precaution supported by evidence in the general population (Depakene Prescribing Information, 2011; Hansen et al., 1995; Craig et al., 1999; Candito et al., 2007).

HIV integrase inhibitor drug class effect on folate transport pathways was not observed in the present study (Figure 6), which is conceptually consistent with the lack of clinical evidence for increased NTD risk by this class of drugs (Vitekta Prescribing Information, 2015, Isentress Prescribing Information, 2019; Stribild Prescribing Information, 2019). Even raltegravir, which was flagged as a potentially clinically-relevant intestinal PCFT inhibitor at the highest 1.2g clinical dose is not known to increase the clinical risk of NTDs or cause birth defects in pre-clinical embryofetal toxicology studies (Isentress Prescribing Information, 2011).

Following the report of potentially increased prevalence of NTD in the ongoing dolutegravir birth surveillance study (Zash et al., 2018), *in vitro* FRα receptor binding experiments were used to demonstrate that dolutegravir is a non-competitive FRα antagonist (Cabrera et al., 2019). Dolutegravir inhibited folic acid binding to FRα up to 44% at concentrations between 16-64 μM, with an apparent IC_{50} of 4.4 μM, where IC_{50} was defined as dolutegravir concentration eliciting 22% inhibition of folic acid binding to FRα, i.e. half of the

maximal inhibitory effect (Cabrera et al., 2019). Considering that Cabrera et al. examined

receptor binding as opposed to functional receptor-mediated endocytosis reported in this study,

the dolutegravir FRα antagonism results (44% inhibition at dolutegravir concentrations 16-64

μM) are in good agreement with 36% inhibition of FRα-mediated folic acid at 37 μM

dolutegravir (Figure 5D and Figure 6). However, Cabrera et al. concluded that dolutegravir

apparent FRα inhibitory potency of 4.4 μM occurred at therapeutic concentrations based on

direct comparison to clinical total plasma concentrations (Table 1; Tivivay Prescribing

Information, 2018). Dolutegravir is highly plasma protein bound (>99%; Table 1; Tivivay

Prescribing Information, 2018), and because only unbound drug is available for pharmacologic

activity (i.e. on- and off-target binding, interactions with transporters and drug metabolizing

enzymes, tissue distribution, etc.), direct comparison of *in vitro* potencies to total plasma

concentrations is not clinically pertinent (Smith et al., 2010). Such a direct *in vitro* to total

plasma comparison may have been possible if 4% albumin were added to the buffer in the FRα

binding study to mimic plasma protein binding, but the comparison was made directly between

in vitro potency in a protein-free buffer and clinical total plasma concentrations for a highly-

bound drug (Cabrera et al., 2019), where clinical unbound plasma concentrations are two orders

of magnitude lower than total concentrations (Table 1; Tivivay Prescribing Information, 2018).

Using the accepted clinical extrapolation approach for the dolutegravir apparent FRα

inhibitory potency of 4.4 μM in the receptor binding assay, $1+Cmax,u/IC_{50} = 1.017$ (Table 1;

FDA, 2017; Cabrera et al., 2019), which is not flagged as clinically-relevant at the level of tissue

distribution ($1+Cmax,u/IC < 1.1$) and renal sparing on apical membrane of renal proximal

tubules ($1+Cmax,u/IC < 1.02$) (FDA, 2017). Since 50% FRα antagonism was not achieved, the

apparent IC_{50} is really an IC_{22} (Cabrera et al., 2019), and it is not accepted practice to use this

18

apparent IC_{50} parameter in clinical extrapolations (FDA, 2017). Applying the present

extrapolation approach for inhibition of folate transport pathways, where the greatest inhibitory

potency ≥25% is used wherever 50% inhibition was not achieved, FRα antagonism IC_{44} = 16 μM

(Cabrera et al., 2019), such that $1+Cmax,u/IC_{50}$ = 1.005 and well below thresholds for potential

clinical significance (Table 1; FDA, 2017; Cabrera et al., 2019).

In the present study, clinical extrapolation of observed *in vitro* inhibitory potency values

were based on established thresholds for clinically-relevant transporter inhibition in the intestine

($Igut/IC_{50} \geq 10$), systemically ($1+Cmax,u/IC_{50} \geq 1.1$), and on apical membrane of renal proximal

tubules ($1+Cmax,u/IC_{50} \geq 1.02$) (FDA, 2017). Although it was validated for transporter-based

drug-drug interactions, the principles should apply to drug-nutrient interactions. This

extrapolation framework is considered the best available and also a conservative approach. As

theoretically expected, intensive study of clinical translation of *in vitro* transport pathway

inhibition demonstrated that the same translational pharmacokinetic principles apply to different

transporter processes located at the same site in the body (i.e. the same principles and thresholds

apply to different transporters localized in the intestine, liver, basolateral or apical membrane of

renal proximal tubules) (International Transporter et al., 2010; Hillgren et al., 2013; FDA, 2017;

Zamek-Gliszczynski et al., 2018). Furthermore, these translational approaches have precedent in

extrapolation of *in vitro* intestinal and systemic thiamine transport by drugs as an alert to drug-

induced Wernicke's disease (Giacomini et al., 2017). Notably, these approaches are based on

IC_{50} values where >50% transport function impairment was observed *in vitro,* and in the present

study any inhibitor concentration associated with the greatest extent of inhibition observed ≥25%

was reported and extrapolated (Figure 6). This ≥25% inhibition level was selected on the basis

that ≥25% cumulative inhibition of folate absorption distribution, and renal tubular reabsorption

19

(sparing) would decrease fetal folate levels >2-fold (Zamek-Gliszczynski et al., 2009; Zamek-Gliszczynski et al., 2013). The present approach of extrapolating any noted *in vitro* inhibition ≥25% of folate transport pathways was deliberately conservative and intended to flag any potential clinical inhibition by the five integrase inhibitor drugs. Even with this conservative ≥25% inhibition approach, the present studies do not support 1) dolutegravir as a clinical inhibitor of the three major folate transport pathways, or 2) clinically-relevant integrase inhibitor drug class effect on folate transport.

The present studies are limited to acute inhibition effects by parent drugs. Parent dolutegravir is the predominant circulating moiety with negligible systemic metabolite exposure (Moss et al., 2015). As such, total radioactivity can be assumed to approximate parent drug concentrations, and relevant tissue-to-blood ratios can be estimated from whole body autoradiography studies in pregnant rats (unpublished GlaxoSmithKline study 2012N137348_00): placenta-to-blood ratio of 0.59 ± 0.10, fetal-to-maternal blood ratio of 0.13 ± 0.02, and kidney-to-blood ratio of 0.42 ± 0.03. The clinical translational framework based on unbound systemic drug levels is supported by these tissue-to-blood ratios, which do not indicate preferential fetal or renal drug partitioning, as well as systemic exposure primarily to parent dolutegravir and not metabolites. However, potential effects of dolutegravir-glucuronide, the major form of dolutegravir in urine (Moss et al., 2015), on folate tubular reabsorption have not been ruled out by the present studies. Furthermore, potential regulation effects on folate transport/metabolism that may occur upon chronic dolutegravir administration remain to be investigated. These would be most relevant to study clinically in terms of blood folate, folate renal clearance, and maternal-to-neonate blood ratio, because clinical translation of in vitro folate transport/metabolism regulation data are not validated.

20

Acknowledgements

Drs. Kim Adkison, Joseph Polli, Dinesh Stanislaus, and Nassrin Payvandi are

acknowledged for their scientific input.

Authorship contribution

Participated in research design: Zamek-Gliszczynski, Zhang, Mudunuru, Taskar, Huang,

Huang, Romach

Conducted experiments: Zhang, Du, Chen

Contributed new reagents and analytic tools: Zhang, Du, Chen, Huang, Huang

Performed data analysis: Zamek-Gliszczynski, Zhang, Mudunuru, Chen, Taskar, Romach

Wrote or contributed to the writing of the manuscript: Zamek-Gliszczynski, Zhang, Mudunuru,

Taskar, Romach

References

Abbott Laboratories. (2011). Depakene (valproic acid) [package insert]. .

Eli Lilly and Company. (2019). Alimta (pemetrexed) [package insert]. .

EMA (2017) – Jylamvo (methotrexate) EPAR – Summary for the public.

Gilead Sciences, Inc. (2015). Vitekta (elvitegravir) [package insert]. .

Gilead Sciences, Inc. (2018). Biktarvy (bictegravir/emtricitabine/tenofovir alafenamide)
[package insert]. .

Gilead Sciences, Inc. (2019). Stribild (elvitegravir/cobicistat/emtricitabine/tenofovir disoproxil
fumarate) [package insert]. .

Merck Sharp & Dohme Corp. (2019). Isentress (raltegravir) [package insert]. .

ViiV Healthcare. (2018). Tivicay (dolutegravir) [package insert]. .

Botto LD, Moore CA, Khoury MJ, and Erickson JD (1999) Neural-tube defects. *N Engl J Med*
341:1509-1519.

Cabrera RM, Souder JP, Steele JW, Yeo L, Tukeman G, Gorelick DA, and Finnell RH (2019)
The Antagonism of Folate Receptor by the Integrase Inhibitor Dolutegravir. *bioRxiv The
Preprint Server for Biology* **https://doi.org/10.1101/576272**.

Candito M, Naimi M, Boisson C, Rudigoz JC, Gaucherand P, Gueant JL, Luton D, and Van
Obberghen E (2007) Plasma vitamin values and antiepileptic therapy: case reports of
pregnancy outcomes affected by a neural tube defect. *Birth Defects Res A Clin Mol
Teratol* **79:**62-64.

Chattopadhyay S, Moran RG, and Goldman ID (2007) Pemetrexed: biochemical and cellular
pharmacology, mechanisms, and clinical applications. *Mol Cancer Ther* **6:**404-417.

Cohen IJ (2017) Neurotoxicity after high-dose methotrexate (MTX) is adequately explained by insufficient folinic acid rescue. *Cancer Chemother Pharmacol* **79:**1057-1065.

Craig J, Morrison P, Morrow J, and Patterson V (1999) Failure of periconceptual folic acid to prevent a neural tube defect in the offspring of a mother taking sodium valproate. *Seizure* **8:**253-254.

Crider KS, Devine O, Hao L, Dowling NF, Li S, Molloy AM, Li Z, Zhu J, and Berry RJ (2014) Population red blood cell folate concentrations for prevention of neural tube defects: Bayesian model. *BMJ* **349:**g4554.

Daly LE, Kirke PN, Molloy A, Weir DG, and Scott JM (1995) Folate levels and neural tube defects. Implications for prevention. *JAMA* **274:**1698-1702.

DeSesso JM and Goeringer GC (1991) Amelioration by leucovorin of methotrexate developmental toxicity in rabbits. *Teratology* **43:**201-215.

FDA US (2017) In Vitro Metabolism - and Transporter- Mediated Drug - Drug Interaction Studies (Pharmacology C ed, pp 45, Office of Communications, FDA CDER, Rockville, MD.

Ford SL, Lou Y, Lewis N, Michalis K, D'Amico R, Spreen W, and Patel P (2019) Effect of rifabutin on the pharmacokinetics of oral cabotegravir in healthy subjects. *Antivir Ther*.

Giacomini MM, Hao J, Liang X, Chandrasekhar J, Twelves J, Whitney JA, Lepist EI, and Ray AS (2017) Interaction of 2,4-Diaminopyrimidine-Containing Drugs Including Fedratinib and Trimethoprim with Thiamine Transporters. *Drug Metab Dispos* **45:**76-85.

Han Y, Mesplede T, and Wainberg MA (2017) Investigational HIV integrase inhibitors in phase I and phase II clinical trials. *Expert Opin Investig Drugs* **26:**1207-1213.

Hansen DK, Grafton TF, Dial SL, Gehring TA, and Siitonen PH (1995) Effect of supplemental folic acid on valproic acid-induced embryotoxicity and tissue zinc levels in vivo. *Teratology* **52:**277-285.

Hillgren KM, Keppler D, Zur AA, Giacomini KM, Stieger B, Cass CE, Zhang L, and International Transporter C (2013) Emerging transporters of clinical importance: an update from the International Transporter Consortium. *Clin Pharmacol Ther* **94:**52-63.

International Transporter C, Giacomini KM, Huang SM, Tweedie DJ, Benet LZ, Brouwer KL, Chu X, Dahlin A, Evers R, Fischer V, Hillgren KM, Hoffmaster KA, Ishikawa T, Keppler D, Kim RB, Lee CA, Niemi M, Polli JW, Sugiyama Y, Swaan PW, Ware JA, Wright SH, Yee SW, Zamek-Gliszczynski MJ, and Zhang L (2010) Membrane transporters in drug development. *Nat Rev Drug Discov* **9:**215-236.

Kancherla V, Wagh K, Johnson Q, and Oakley GP, Jr. (2018) A 2017 global update on folic acid-preventable spina bifida and anencephaly. *Birth Defects Res* **110:**1139-1147.

Kavathiya K, Gurjar M, Patil A, Naik M, Noronha V, Joshi A, Gota V, and Prabhash K (2017) A Comparative Pharmacokinetic Study of 2 Pemetrexed Formulations in Indian Adult Chemonaive Patients With Adenocarcinoma Stage III/IV Non-Small Cell Lung Cancer. *Clin Pharmacol Drug Dev* **6:**234-239.

Kim CH, Park YS, Chung KN, and Elwood PC (2004) Sorting of the human folate receptor in MDCK cells. *J Biochem Mol Biol* **37:**362-369.

Kneuer C, Honscha KU, and Honscha W (2005) Rat reduced-folate carrier-1 is localized basolaterally in MDCK kidney epithelial cells and contributes to the secretory transport of methotrexate and fluoresceinated methotrexate. *Cell Tissue Res* **320:**517-524.

Matherly LH, Hou Z, and Deng Y (2007) Human reduced folate carrier: translation of basic biology to cancer etiology and therapy. *Cancer Metastasis Rev* **26:**111-128.

Mauritz, Milstein S, Kapatos G, Levine RA, and Shane B (2001) *Chemisty and Biology of Pteridines and Folates*. Springer US, Bethesda, Maryland.

Moss L, Wagner D, Kanaoka E, Olson K, Yueh YL, and Bowers GD (2015) The comparative disposition and metabolism of dolutegravir, a potent HIV-1 integrase inhibitor, in mice, rats, and monkeys. *Xenobiotica* **45:**60-70.

Nakai Y, Inoue K, Abe N, Hatakeyama M, Ohta KY, Otagiri M, Hayashi Y, and Yuasa H (2007) Functional characterization of human proton-coupled folate transporter/heme carrier protein 1 heterologously expressed in mammalian cells as a folate transporter. *J Pharmacol Exp Ther* **322:**469-476.

Rizk ML, Krishna R, Schulz V, ten Bruggencate-Broeders J, Larson P, and Wenning L (2014) A Multiple Dose Study of Raltegravir Formulations. *CROI* *http://wwwcroiconferenceorg/sessions/multiple-dose-study-raltegravir-ral-formulations*.

Seideman P, Beck O, Eksborg S, and Wennberg M (1993) The pharmacokinetics of methotrexate and its 7-hydroxy metabolite in patients with rheumatoid arthritis. *Br J Clin Pharmacol* **35:**409-412.

Smith DA, Di L, and Kerns EH (2010) The effect of plasma protein binding on in vivo efficacy: misconceptions in drug discovery. *Nat Rev Drug Discov* **9:**929-939.

Solanky N, Requena Jimenez A, D'Souza SW, Sibley CP, and Glazier JD (2010) Expression of folate transporters in human placenta and implications for homocysteine metabolism. *Placenta* **31:**134-143.

Zamek-Gliszczynski MJ, Kalvass JC, Pollack GM, and Brouwer KL (2009) Relationship between drug/metabolite exposure and impairment of excretory transport function. *Drug Metab Dispos* **37:**386-390.

Zamek-Gliszczynski MJ, Lee CA, Poirier A, Bentz J, Chu X, Ellens H, Ishikawa T, Jamei M, Kalvass JC, Nagar S, Pang KS, Korzekwa K, Swaan PW, Taub ME, Zhao P, Galetin A, and International Transporter C (2013) ITC recommendations for transporter kinetic parameter estimation and translational modeling of transport-mediated PK and DDIs in humans. *Clin Pharmacol Ther* **94:**64-79.

Zamek-Gliszczynski MJ, Taub ME, Chothe PP, Chu X, Giacomini KM, Kim RB, Ray AS, Stocker SL, Unadkat JD, Wittwer MB, Xia C, Yee SW, Zhang L, Zhang Y, and International Transporter C (2018) Transporters in Drug Development: 2018 ITC Recommendations for Transporters of Emerging Clinical Importance. *Clin Pharmacol Ther* **104:**890-899.

Zash R, Makhema J, and Shapiro RL (2018) Neural-Tube Defects with Dolutegravir Treatment from the Time of Conception. *N Engl J Med* **379:**979-981.

Zhao R, Diop-Bove N, Visentin M, and Goldman ID (2011) Mechanisms of membrane transport of folates into cells and across epithelia. *Annu Rev Nutr* **31:**177-201.

Footnotes

This study was funded by ViiV Healthcare. Authors declare no conflicts of interest beyond

employment noted in affiliations.

Figure Legends

Figure 1. Proton-coupled folate transporter (PCFT), reduced folate carrier (RFC), and folate receptor α (FRα)-mediated endocytosis in folate absorption, distribution, and renal tubular reabsorption (Kim et al., 2004; Solanky et al., 2010; Zhao et al., 2011). GFR = glomerular filtration rate, CSF = cerebrospinal fluid, PT = renal proximal tubule.

Figure 2. Diagram of experimental setup for (A) PCFT transport, (B) RFC transport, and (C) FRα-mediated endocytosis studies. TA = test article, LDH = lactate dehydrogenase.

Figure 3. PCFT transport of 10 nM [^{3}H]-folic acid in the presence of (A) assay positive control inhibitor, bromosulfophthalein (nominal concentrations and IC_{50}), (B) clinical positive control, methotrexate, (C) clinical negative control, valproic acid, (D) dolutegravir, (E) cabotegravir, (F) bictegravir, (G) elvitegravir, and (H) raltegravir. Black symbols represent PCFT [^{3}H]-folic acid uptake activity at various test article concentrations, solid black line is IC_{50} curve fit with IC_{50} estimate shown wherever >50% inhibition was observed, red square symbols (B-H) denote PCFT activity in the presence of assay positive control (bromosulfophthalein at 300 μM nominal concentration), dashed blue line (B-H) represents 100% PCFT activity (i.e. no inhibition). All test article concentrations were determined experimentally at the end of the experiment, except bromosulfophthalein concentrations are nominal. Mean ± S.D., n = 4.

Figure 4. RFC transport of 0.5 μM [^{3}H]-methotrexate in the presence of (A) assay positive control inhibitor, pemetrexed (nominal concentrations and IC_{50}), (B) clinical positive control, methotrexate, (C) clinical negative control, valproic acid, (D) dolutegravir, (E) cabotegravir, (F)

bictegravir, (G) elvitegravir, and (H) raltegravir. Black symbols represent RFC [^{3}H]-methotrexate uptake activity at various test article concentrations, solid black line is IC$_{50}$ curve fit with IC$_{50}$ estimate shown wherever >50% inhibition was observed, red square symbols (B-H) denote RFC activity in the presence of assay positive control (pemetrexed at 1 mM nominal concentration), dashed blue line (B-H) represents 100% RFC activity (i.e. no inhibition). All test article concentrations were determined experimentally at the end of the experiment, except pemetrexed concentrations are nominal. Mean ± S.D., n = 4.

Figure 5. FRα-mediated endocytosis of 50 nM [^{3}H]-folic acid in the presence of (A) assay positive control inhibitor, pemetrexed (nominal concentrations and IC$_{50}$), (B) clinical positive control, methotrexate, (C) clinical negative control, valproic acid, (D) dolutegravir, (E) cabotegravir, (F) bictegravir, (G) elvitegravir, and (H) raltegravir. Black symbols represent FRα-mediated [^{3}H]-folic acid uptake activity at various test article concentrations, solid black line is IC$_{50}$ curve fit with IC$_{50}$ estimate shown wherever >50% inhibition was observed, red square symbols (B-H) denote FRα activity in the presence of assay positive control (pemetrexed at 300 μM nominal concentration), dashed blue line (B-H) represents 100% FRα activity (i.e. no inhibition). All test article concentrations were determined experimentally at the end of the experiment, except pemetrexed concentrations are nominal. Mean ± S.D., n = 4.

Figure 6. Clinical extrapolation summary for PCFT, RFC, and FRα inhibition in folate absorption, distribution, and renal sparing.

Table 1. Drug parameters relevant for clinical extrapolation of *in vitro* transport inhibition.

Drug	MW	Dose	Cmax	fu	Cmax,u	Igut	Reference
	(g/mol)	(mg)	(μM)		(μM)	(μM)	
dolutegravir	441.36	50	8.32[a]	0.01	0.08[a]	453.14	(ViiV Healthcare, 2018)
cabotegravir	427.33	30	14.88	0.01	0.15	280.81	(Ford et al., 2019)
bictegravir	449.38	50	13.69	0.01	0.14	445.06	(Gilead, 2018)
raltegravir	482.51	400	4.50	0.17	0.76	3315.99	(Merck, 2019)
raltegravir	482.51	1200	22.56	0.17	3.84	9947.98	(Rizk et al., 2014)
elvitegravir	447.88	85	2.68[b]	0.02	0.05[b]	759.13	(Gilead, 2015)
elvitegravir	447.88	150	3.35[b]	0.02	0.07[b]	1339.64	(Gilead, 2015)
methotrexate	454.44	10	0.57	0.5	0.28	88.02	(EMA, 2017)
methotrexate (IV)	454.44	15	3.80	0.5	1.90	N/A	(Seideman et al., 1993)
pemetrexed (IV)	597.49	500 mg/m²	189.12	0.19	35.93	N/A	(Kavathiya et al., 2017)

IV = intravenous (oral administration in all cases, unless IV noted), MW = molecular weight, Cmax = maximal plasma concentration, fu = plasma fraction unbound, Cmax,u = unbound Cmax (i.e. Cmax * fu), Igut = theoretical gut concentration (oral dose / 250 mL) or highest soluble aqueous concentration, N/A = not applicable (IV administration)
[a]Most commonly used 50mg QD regimen; 50mg BID Cmax = 9.4 μM and Cmax,u = 0.09 μM (ViiV Healthcare, 2018), BID dosing not impact extrapolation values or results in Figure 6
[b]not cobicistat boosted, 150mg dose cobicistat-boosted Cmax = 3.8 μM and Cmax,u = 0.08 μM (Gilead, 2019); cobicistat boosting does not impact extrapolation values or results in Figure 6
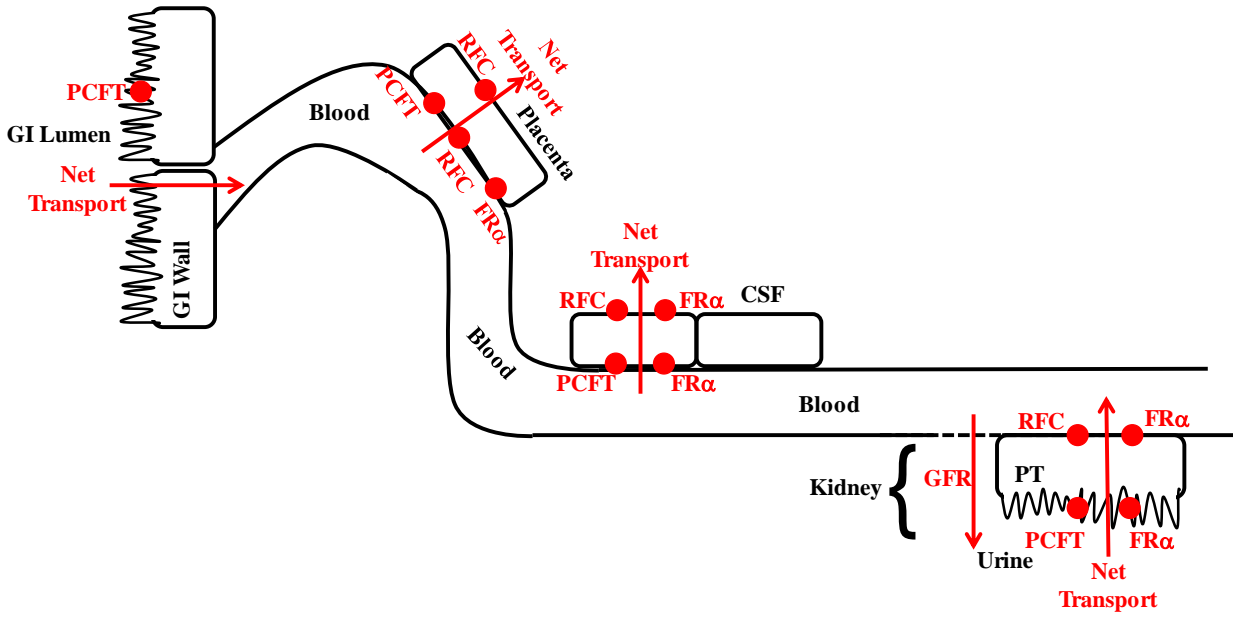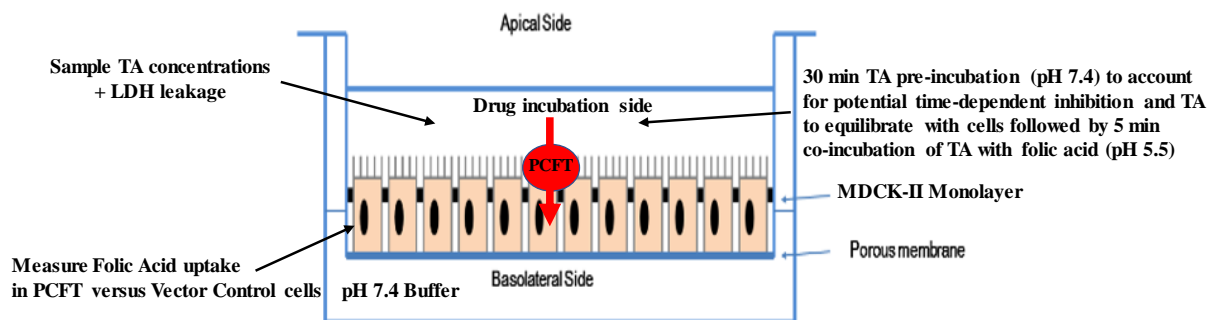
Figure 1.

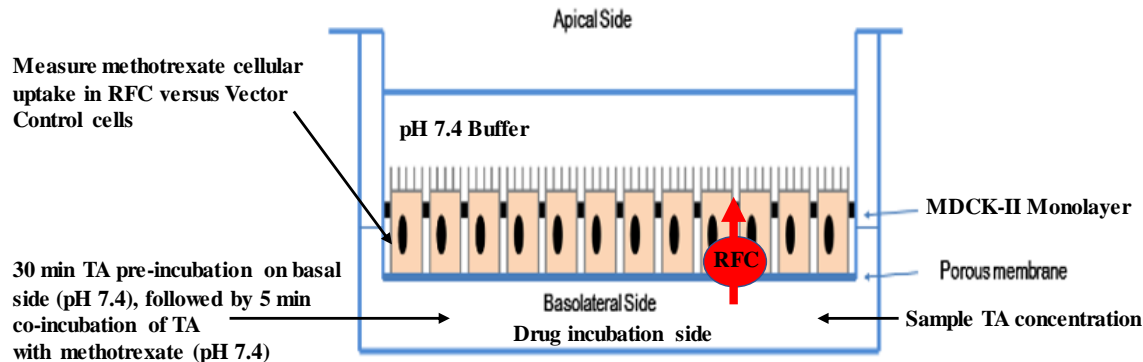Figure 2.

A.

SCHEMATIC OF PCFT TRANSPORT EXPERIMENTS

B.

SCHEMATIC OF RFC TRANSPORT EXPERIMENTS

C.

SCHEMATIC OF FRα ENDOCYTOSIS EXPERIMENTS
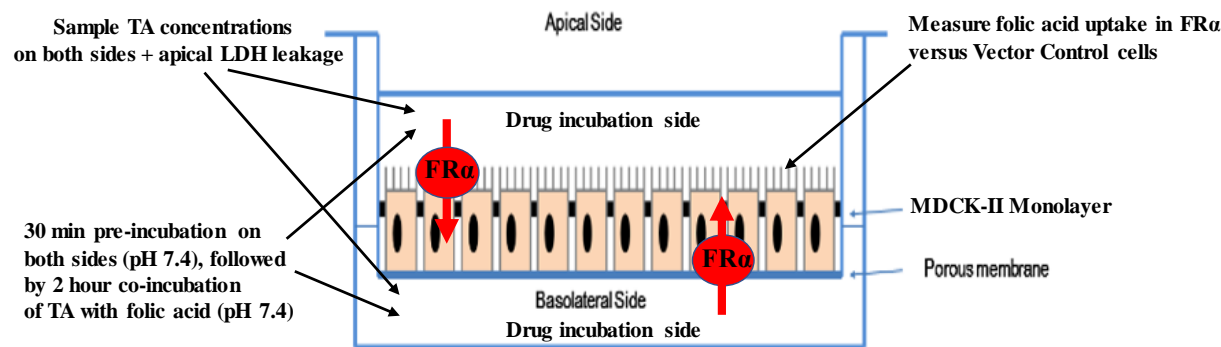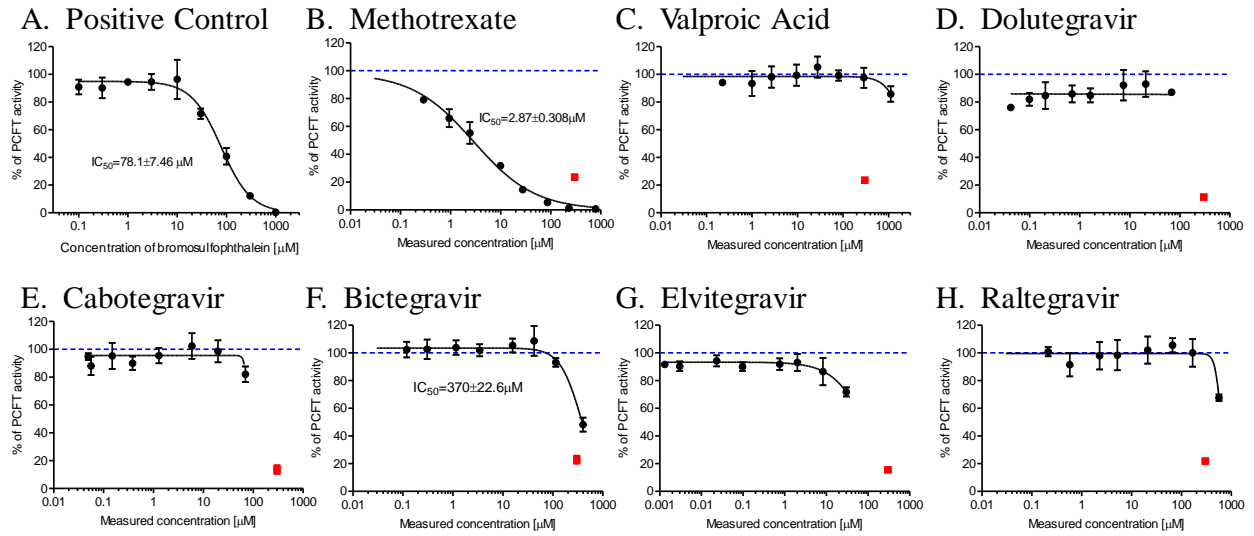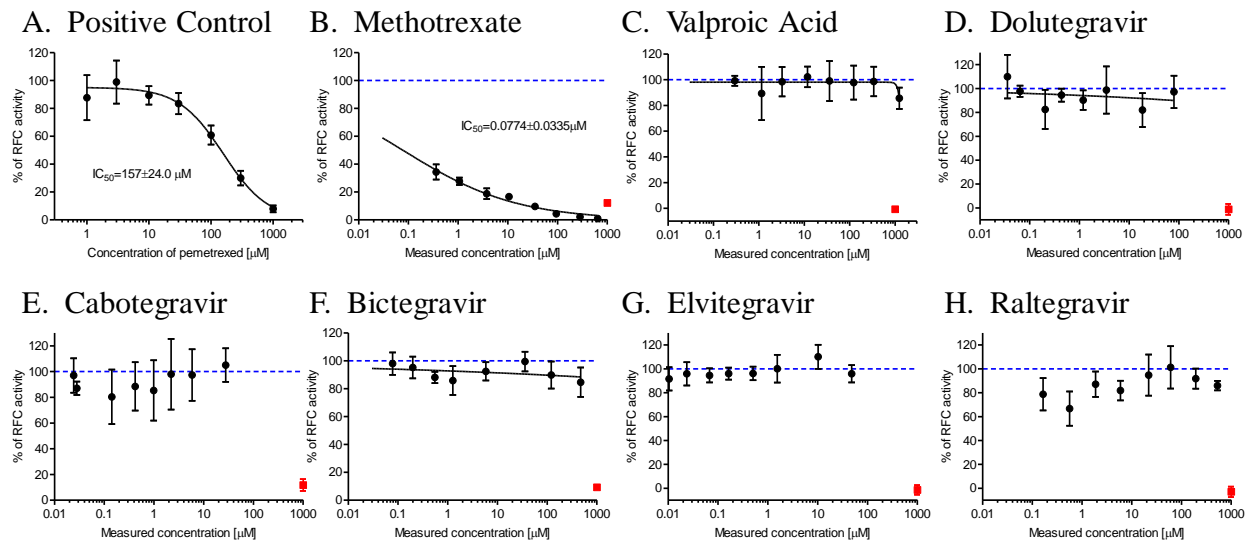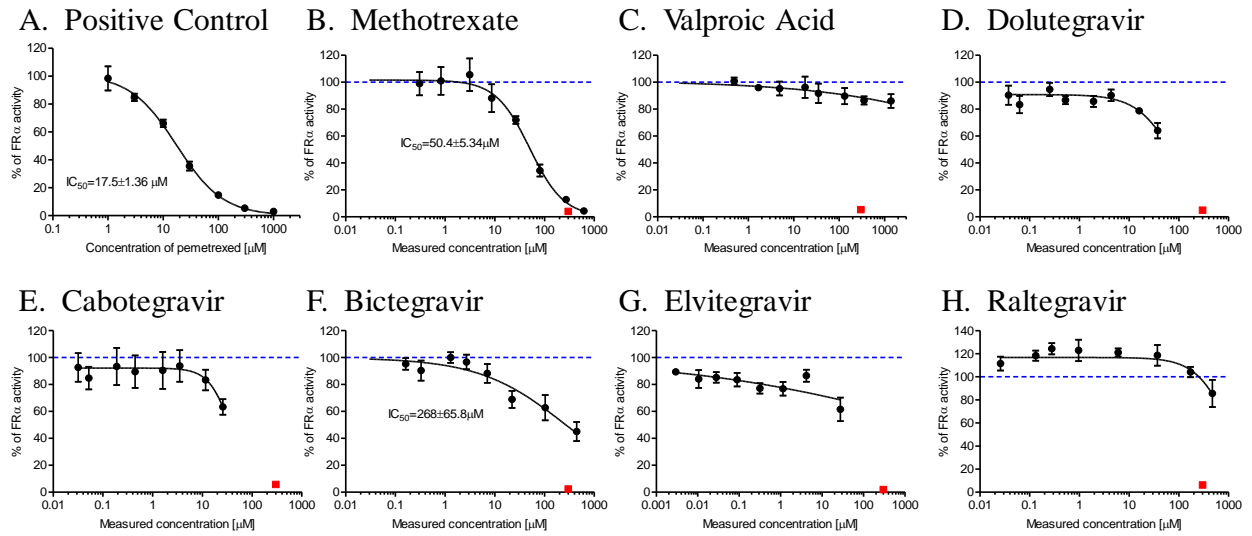
Figure 3.

Figure 4.

Figure 5.

Figure 6.

Drug	Inhibition* (IC_{50} or $IC_{\geq 25\%}$)						
	PCFT			RFC		FRα	
	Absorption	Distribution	Renal sparing	Distribution	Renal sparing	Distribution	Renal sparing
dolutegravir						IC_{36} = 37 µM $1+C_{max\,u}/IC_{36}$ = 1.002 <1.1	IC_{36} = 37 µM $1+C_{max\,u}/IC_{36}$ = 1.002 <1.02
cabotegravir						IC_{37}= 25.8 µM $1+C_{max\,u}/IC_{37}$ = 1.006 <1.1	IC_{37}= 25.8 µM $1+C_{max\,u}/IC_{37}$ = 1.006 <1.02
bictegravir	IC_{50} = 370 µM I_{gut}/IC_{50} = 0.6 <10	IC_{50} = 370 µM $1+C_{max\,u}/IC_{50}$= 1.0004 <1.1	IC_{50} = 370 µM $1+C_{max\,u}/IC_{50}$ = 1.0004 <1.02			IC_{50} = 268 µM $1+C_{max\,u}/IC_{50}$ = 1.0005 <1.1	IC_{50} = 268 µM $1+C_{max\,u}/IC_{50}$ = 1.0005 <1.02
raltegravir	IC_{32} = 564 µM I_{gut}/IC_{32} = 17.6 >10	IC_{32} = 564 µM $1+C_{max\,u}/IC_{32}$ = 1.007 <1.1	IC_{32} = 564 µM $1+C_{max\,u}/IC_{32}$ = 1.007 <1.02				
elvitegravir	IC_{28} = 30 µM I_{gut}/IC_{28} = 0.02 <10	IC_{28} = 30 µM $1+C_{max\,u}/IC_{28}$ = 1.002 <1.1	IC_{28} = 30 µM $1+C_{max\,u}/IC_{28}$ = 1.002 <1.02				
methotrexate	IC_{50} = 2.9 µM I_{gut}/IC_{50} = 31 >10	IC_{50} = 2.9 µM $1+C_{max,u}/IC_{50}$ = 1.7 >1.1	IC_{50} = 2.9 µM $1+C_{max,u}/IC_{50}$ = 1.7 >1.02	IC_{50} = 0.08 µM $1+C_{max,u}/IC_{50}$ = 50 >1.1	IC_{50} = 0.08 µM $1+C_{max,u}/IC_{50}$ = 50 >1.1	IC_{50} = 50.4 µM $1+C_{max\,u}/IC_{50}$ = 1.07 <1.1	IC_{50}= 50.4 µM $1+C_{max,u}/IC_{50}$ = 1.07 >1.02
pemetrexed (nominal conc)	IV Dose - N/A	IC_{50} - N/D	IC_{50} - N/D	IC_{50} = 157 µM $1+C_{max,u}/IC_{50}$ = 1.2 >1.1	IC_{50} = 157 µM $1+C_{max,u}/IC_{50}$ = 1.2 >1.1	IC_{50} = 17.5 µM $1+C_{max,u}/IC_{50}$ = 3.1 >1.1	IC_{50} = 17.5 µM $1+C_{max,u}/IC_{50}$ = 3.1 >1.02
valproic acid						IC_{15} = 1380 µM[1]	IC_{15}= 1380 µM[1]

☐   No *in vitro* inhibition up to the highest soluble concentration

🟩   *In vitro* inhibition observed – **NOT** clinically relevant (FDA, 2017)

🟥   *In vitro* inhibition observed and **POTENTIAL CLINICAL RISK OF INHIBITION** (FDA, 2017)

IV dose - N/A (Not Applicable) or IC_{50} N/D (Not Determined)

*None of the reported inhibitory data are an artifact of cytotoxicity (see Supplemental Table 3)

[1]Did not meet pre-defined ≥25% inhibition threshold for FRα-mediated endocytosis, but a consistent trend of apparently concentration-dependent inhibition was noted up to 15% at the highest concentration tested

Cmax,u = unbound maximal plasma concentration, Igut = theoretical gut concentration (oral dose / 250 mL) or highest soluble aqueous concentration, IC = inhibitory concentration

Clinical Extrapolation of the Effects of Dolutegravir and Other HIV Integrase Inhibitors on Folate Transport Pathways

Maciej J. Zamek-Gliszczynski, Xuexiang Zhang, Jennypher Mudunuru, Yewei Du, Jian-Lu Chen, Kunal S. Taskar, Jane Huang, Yong Huang, and Elizabeth H. Romach

GlaxoSmithKline, Collegeville, PA, USA (MJZ-G, JM), and Ware, UK (KST); BioIVT, Santa Clara, CA, USA (XZ, YD, J-LC, JH, YH); ViiV Healthcare, RTP, NC, USA (EHR)

Supplemental Methods 1: LC-MS/MS bioanalytical method summary.

Sample preparation

In PCFT assay, eight concentrations of the test article were applied to the apical side of columns 3 through 10 in a 96-well cell plate transfected with a control vector in Rows A to D, and PCFT in Rows E to H. At the end of 5 min incubation, 20 µL samples were taken from the apical side and transferred to the corresponding wells in a 96-well sample plate preloaded with 180 µL internal standard in 50% acetonitrile (acetonitrile:H_2O=1:1). Samples were frozen at -80ºC for later detection.

In RFC assay, eight concentrations of the test article were applied to the basal side of columns 3 through 10 in a 96-well cell plate transfected with a control vector in Rows A to D, and RFC in Rows E to H. At the end of 5 min incubation, 20 µL samples were taken from the basal side and transferred to the corresponding wells in a 96-well sample plate preloaded with 180 µL internal standard in 50% acetonitrile (acetonitrile:H_2O=1:1). Samples were frozen at -80ºC for later detection.

In FRα assay, eight concentrations of the test article were applied to both sides of columns 3 through 10 in a 96-well cell plate transfected with a control vector in Rows A to D, and FRα in Rows E to H. At the end of 120 min incubation, 20 µL samples were taken from the apical side and basal side of Rows E-H and transferred to Rows A to D, and E to H, respectively, in a 96-well sample plate preloaded with 180 µL internal standard in 50% acetonitrile (acetonitrile:H_2O=1:1). Samples were frozen at -80ºC for later detection. Rows A-D in the cell plate (cells transfected with a control vector) were not sampled.

LC-MS/MS analytical conditions for dolutegravir, cabotegravir, bictegravir, elvitegravir, raltegravir, methotrexate, and valproic acid

1. Equipment

LC model (Shimadzu)	Shimadzu LC-20AD, and Shimadzu SIL-20A
	Analyst 1.6.2. software for instrument control and data analysis
	API4000 triple quadrupole MS
MS model (AB Sciex)	Analyst 1.6.2. software for instrument control and data analysis

2. LC Conditions

Column type	Kinetex Polar-C18, 2.6 µm particle size, 3.0 x 50 mm
Eluent A	5% ACN in H_2O, w/ 0.1% formic acid and 5mM ammonium formate
Eluent B	95% ACN in H_2O, w/ 0.1% formic acid and 5mM ammonium formate
Flow rate	800 µL/min
Column temperature	Room temperature
Injection volume	2 µL

Gradient

time (min)	A (%)	B (%)
BIC, CAB, DOL, EVT, MTX		
0	98	2
0.2	60	40
0.4	20	80
0.8	0	100
1.2	0	100
1.25	98	2
2	98	2
RAL, VPA		
0	100	0
0.2	98	2
0.4	20	80
0.8	0	100
1.2	0	100
1.25	100	0
2	100	0

3. MS parameters

bictegravir, cabotegravir, dolutegravir, elvitegravir, and methotrexate:

Ionization:	ESI(+)
Scan type	MRM
Ionspray Voltage	4500 V
Ion Source gas 1	50 psi
Ion Source gas 2	50 psi
Curtain gas	20 psi
Temperature	500 °C
Resolution Q_1	Unit
Resolution Q_3	Unit
DP	50
EP	10

raltegravir and valproic acid:

Ionization:	ESI(-)
Scan type	MRM
Ionspray Voltage	4500 V
Ion Source gas 1	50 psi

Ion Source gas 2	50 psi					
Curtain gas	20 psi					
Temperature	500 °C					
Resolution Q_1	Unit					
Resolution Q_3	Unit					
DP	50					
EP	10					

	Q1 mass (Da)	Q3 mass (Da)	Dwell time (msec)	DP	CE	CXP
bictegravir	450.2	289.1	150	116	39	18
cabotegravir	406.3	127.0	150	106	37	10
dolutegravir	420.2	277.2	150	111	35	16
elvitegravir	448.2	430.2	150	81	29	12
methotrexate	455.3	308.2	150	90	40	12
IS_Carbutamide(+)	270.0	156.2	150	50	25	12
raltegravir	443.2	315.9	150	-95	-24	-9
valproic Acid	142.9	142.9	150	-55	-8	-11
IS_Carbutamide(-)	269.9	171.0	150	-40	-20	-15

Internal standard (IS): Carbutamide

Retention time(min.):

|	
bictegravir	1.32
cabotegravir	1.29
dolutegravir	1.30
elvitegravir	1.45
methotrexate	1.18
raltegravir	1.34
valproic acid	1.32
IS_Cabutamide (+)	1.26
IS_Cabutamide (-)	1.32/1.36

LOD for BIC, CAB, DUL, EVT, MTX, RAL	0.5 ~ 1 nM
LOD for valproic acid	100 nM

Matrix: HBSS+50% Acetonitrile

Supplemental Figure 2: Functional verification of optimized folate *in vitro* transport assays.
PCFT transport of 10 nM [³H]-folic acid (A). RFC transport of 0.5 µM [³H]-methotrexate (B).
FRα-mediated endocytosis of 50 nM [³H]-folic acid (C). Note all inhibitor concentrations and
IC_{50} values are nominal. Mean ± S.D., n = 4.
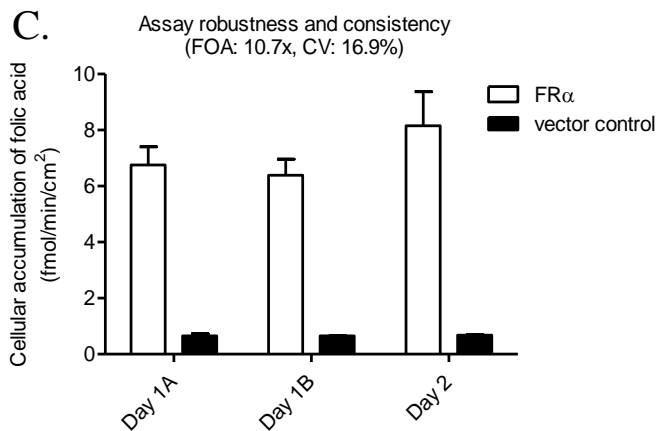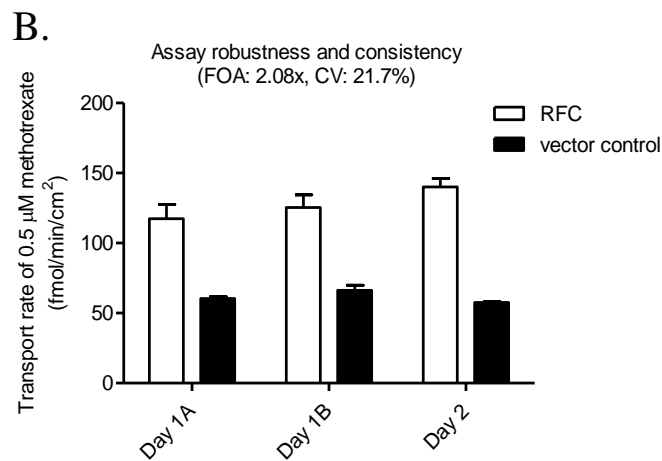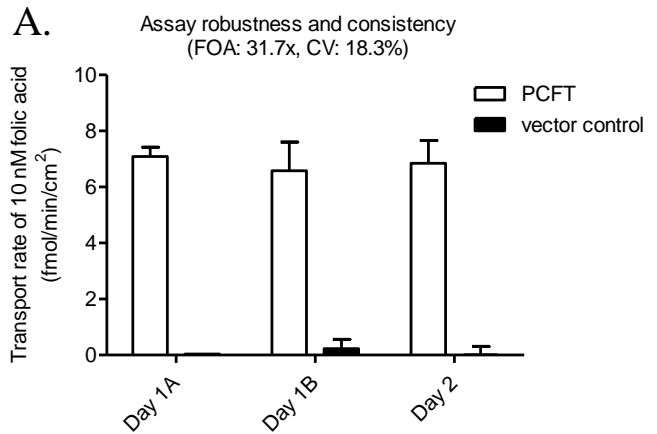
Supplemental Table 3: Evaluation of cytotoxicity by lactate dehydrogenase (LDH) leakage.

To evaluate the possibility that inhibition observed in the FRα endocytosis assays (longest incubation duration on both apical and basolateral sides) was an artifact of cytotoxicity, LDH release was investigated in FRα-expressing and control cells at the two highest test article concentrations. As this was the longest incubation of cells and from both sides, a negative cytotoxicity results in this assay was deemed adequate to address cytotoxicity in PFCT and RFC assays (35 min vs 2.5 h incubation and only from apical or basal side vs both). Only elvitegravir exhibited statistically significant >12.5% cytotoxicity in the FRα-expressing cells at the top two tested concentrations (Supplemental Table 3.1). However, elvitegravir cytotoxicity was not observed under the incubation conditions of the PCFT assay, where inhibition of this transporter was observed at the two highest elvitegravir concentrations, and which cannot be attributed to cytotoxicity (Supplemental Table 3.2).

Supplemental Table 3.1. LDH release in vector control and FRα-expressing cells following incubation with test articles.

Treatment	Concentration (μM)	Absorbance-Blank (FRα receptor)			Absorbance-Blank (vector control)			% Cytotoxicity (FRα receptor)			% Cytotoxicity (vector control)		
Vehicle		641	±	64	1,005	±	187	0.0	±	0.0	0.0	±	0.0
dolutegravir	15.9	875	±	128	1,350	±	102	2.7	±	1.5	4.5	±	1.4
dolutegravir	37.3	924	±	153	1,036	±	99	3.3	±	1.8	0.4	±	1.3
cabotegravir	11.6	1,189	±	204	1,047	±	242	6.3	±	2.4	0.6	±	3.2
cabotegravir	25.8	1,033	±	144	1,125	±	398	4.5	±	1.7	1.6	±	5.2
bictegravir	103	1,691	±	36	1,495	±	462	12.1	±	0.7	6.4	±	6.1
bictegravir	442	1,479	±	117	1,462	±	1,020	9.7	±	1.4	5.9	±	13.4
elvitegravir	4.18	2,975	±	474	809	±	193	26.9	±	5.6*	-2.6	±	2.5
elvitegravir	27.6	1,817	±	233	1,925	±	682	13.6	±	2.8*	12.1	±	8.9
raltegravir	171	1,738	±	645	916	±	167	12.7	±	7.5	-1.2	±	2.1
raltegravir	472	1,134	±	114	1,028	±	126	5.7	±	1.3	0.3	±	1.6
valproic acid	352	1,150	±	111	1,031	±	79	5.9	±	1.3	0.3	±	1.0
valproic acid	1,380	1,192	±	485	7,626	±	4,240	6.5	±	5.6	86.9	±	55.7
methotrexate	271	717	±	186	710	±	250	0.9	±	2.1	-3.9	±	3.3
methotrexate	616	1,200	±	80	1,177	±	458	6.4	±	1.0	2.3	±	6.0
1% Triton-X 100		9,312	±	393	8,627	±	592	100	±	6.4*	100	±	8.9*

% of toxicity was calculated assuming vehicle was 0% and 1% Triton-X was 100%.
* >12.5% cytotoxicity, which is significantly different from vehicle by t-test with Bonferroni's correction. Mean ± S.D., n = 3.

Supplemental Table 3.2. LDH release in vector control and PCFT-expressing cells after incubation with elvitegravir.

Treatment	Concentration (μM)	Absorbance-Blank (PCFT)			Absorbance-Blank (vector control)			% Cytotoxicity (PCFT)			% Cytotoxicity (vector control)		
Vehicle		1,547	±	319	1,279	±	160	0.0	±	0.0	0.0	±	0.0
elvitegravir	8.24	1,210	±	217	1,968	±	223	-3.9	±	2.5	7.8	±	2.5
elvitegravir	30.0	701	±	168	1,088	±	155	-9.8	±	1.9	-2.2	±	1.7
1% Triton-X100		10,140	±	95	10,160	±	125	100	±	1.5*	100	±	1.9*

% of toxicity was calculated assuming vehicle was 0% and 1% Triton-X was 100%.
* >12.5% cytotoxicity, which is significantly different from vehicle by t-test with Bonferroni's correction. Mean ± S.D., n = 3.